ACS ENVIRONMENTAL Au
AN OPEN ACCESS JOURNAL OF THE AMERICAN CHEMICAL SOCIETY

pubs.acs.org/environau
Article

Liquid–Liquid Phase Separation Can Drive Aerosol Droplet Growth in Supersaturated Regimes

Kotiba Malek, Kanishk Gohil, Esther A. Olonimoyo, Nahin Ferdousi-Rokib, Qishen Huang, Kiran R. Pitta, Lucy Nandy, Katelyn A. Voss, Timothy M. Raymond,* Dabrina D Dutcher,* Miriam Arak Freedman,* and Akua Asa-Awuku*

Cite This: ACS Environ. Au 2023, 3, 348–360
Read Online

ACCESS | Metrics & More | Article Recommendations | Supporting Information

ABSTRACT: It is well known that atmospheric aerosol size and composition impact air quality, climate, and health. The aerosol composition is typically a mixture and consists of a wide range of organic and inorganic particles that interact with each other. Furthermore, water vapor is ubiquitous in the atmosphere, in indoor air, and within the human body's respiratory system, and the presence of water can alter the aerosol morphology and propensity to form droplets. Specifically, aerosol mixtures can undergo liquid–liquid phase separation (LLPS) in the presence of water vapor. However, the experimental conditions for which LLPS impacts water uptake and the subsequent prediction of aerosol mixtures are poorly understood. To improve our understanding of aerosol mixtures and droplets, this study explores two ternary systems that undergo LLPS, namely, the 2MGA system (sucrose + ammonium sulfate + 2-methylglutaric acid) and the PEG1000 system (sucrose + ammonium sulfate + polyethylene glycol 1000). In this study, the ratio of species and the O:C ratios are systematically changed, and the hygroscopic properties of the resultant aerosol were investigated. Here, we show that the droplet activation above 100% RH of the 2MGA system was influenced by LLPS, while the droplet activation of the PEG1000 system was observed to be linearly additive regardless of chemical composition, O:C ratio, and LLPS. A theoretical model that accounts for LLPS with O:C ratios was developed and predicts the water uptake of internally mixed systems of different compositions and phase states. Hence, this study provides a computationally efficient algorithm to account for the LLPS and solubility parameterized by the O:C ratio for droplet activation at supersaturated relative humidity conditions and may thus be extended to mixed inorganic–organic aerosol populations with unspeciated organic composition found in the ambient environment.

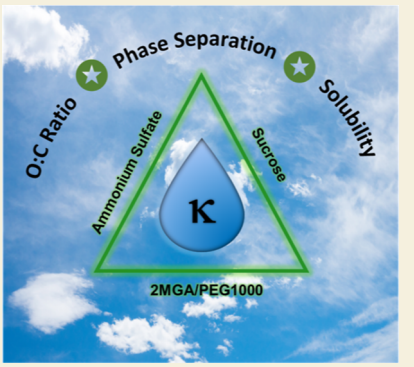

KEYWORDS: *hygroscopicity, organic aerosols, particle morphology, phase separation, aerosol mixtures*

1. INTRODUCTION

Aerosol particles are tiny solid or liquid particles suspended in the air, and they play a key role in health, climate, and air quality.[1] They can be emitted directly into the air from human activities, such as burning fossil fuels, biomass, and agricultural waste, or from natural sources, such as dust storms, oceans, and volcanos.[1,2] They are also formed via complex atmospheric chemical oxidation and nucleation.[3] As such, aerosols impact air quality and have major consequences with regard to human health.[4]

Small aerosols penetrate deep into the humid respiratory system and cause adverse health effects.[5,6] Exposure to fine particulate matter (PM2.5) is associated with increased hospital admissions due to cardiovascular and respiratory diseases.[6−8] In addition to their impact on health, aerosols in humid environments can form haze and smog through their ability to absorb and scatter light, leading to visibility impairment.[9,10] For example, a study conducted by Zhang et al. investigated the effects of aerosols on visibility in various cities in northwestern China.[9] The study reports that increased aerosol concentration leads to decreased visibility, with PM2.5 being the primary contributor to the visibility reduction.[9] The magnitude of their impact on health, air quality, and the climate is dependent on aerosol composition and size.[5,11] Furthermore, aerosol physical composition can be modified in the presence of water, and such effects have traditionally been studied in the context of effects of aerosols on the climate.

The aerosol effects on the climate stem from their ability to impact radiative forcing either directly—through their ability to absorb or reflect radiation—or indirectly—by acting as cloud condensation nuclei (CCN), which enables them to take up water and form cloud droplets.[1,2] The CCN activity of

Received: May 2, 2023
Revised: July 31, 2023
Accepted: July 31, 2023
Published: September 11, 2023

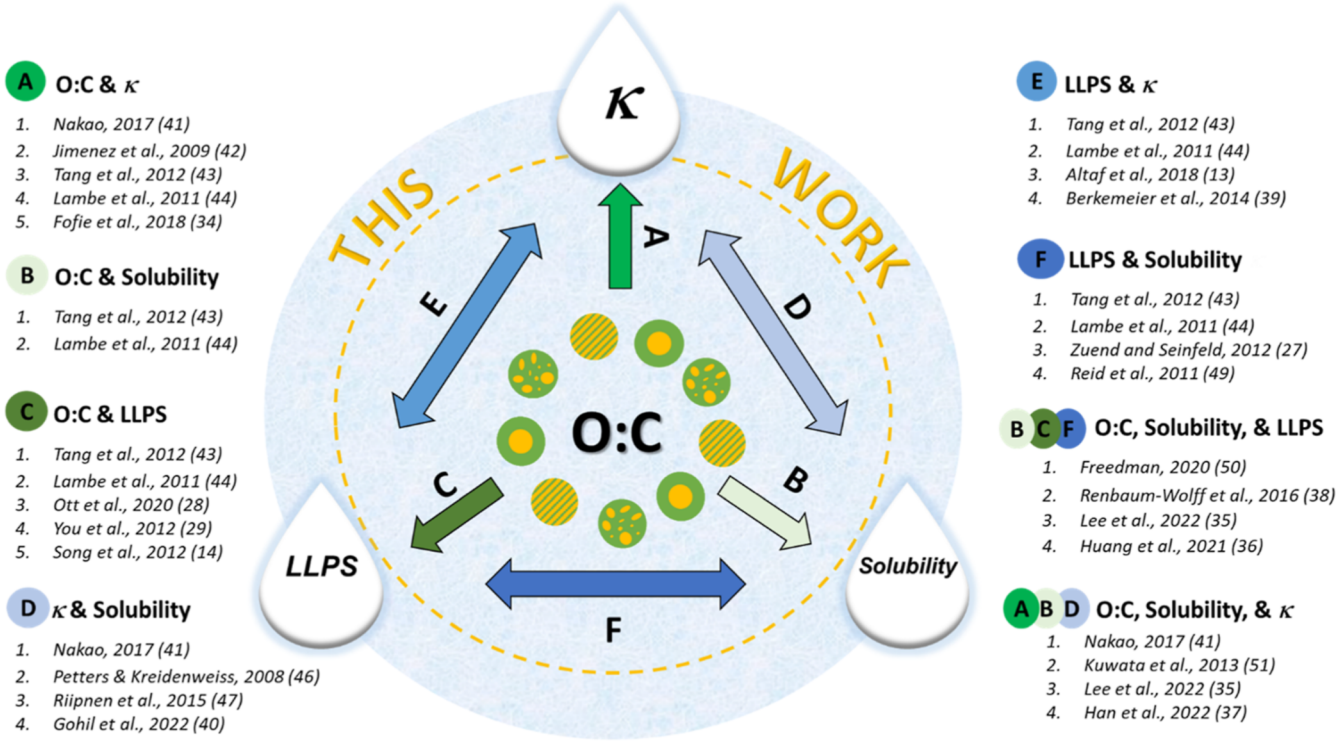

Figure 1. Review of known experimental trends between aerosol physicochemical factors (hygroscopicity, solubility, and LLPS) with the O:C ratio. This work provides a comprehensive analysis and method to incorporate all four factors with experimental data. LLPS: liquid−liquid phase separation; κ: single hygroscopicity parameter; and O:C: oxygen-to-carbon ratio.

aerosols remains uncertain in climate science due to the complexity of their chemistry.[1,12] For instance, the CCN activity of aerosols depends on many factors, including chemical composition, physical state, morphology, and size.[1,2,13−15] These factors will influence the amount of water absorbed, which will consequently affect the scattering or absorption of light, reduction in visibility, and human respiration. Hence, insights into the effect of these variables on aerosol−cloud interactions, water uptake, and droplet formation would directly enhance our understanding of cloud microphysics and, as a result, improve our knowledge of air quality and the climate.[11,16]

Atmospheric aerosols consist of a mixture of organic and inorganic components.[1,17−19] Particle formation and atmospheric chemical processes commonly result in the formation of internally mixed organic−inorganic particles.[17,19,20] Such internally mixed systems can exist in different phase states depending on aerosol composition (type of organic and inorganic salts), average oxygen-to-carbon (O:C) ratio, and environmental conditions [temperature and relative humidity (RH)].[14,21−25] An internal organic−inorganic mixture can also undergo liquid−liquid phase separation (LLPS).[14,21,26−29] Hence, knowledge of the aerosol chemical composition and their subsequent mixtures can improve water uptake predictions and has been the focus of several studies (including but not limited to Hodas et al.,[30] Altaf et al.,[13] Razafindrambinina et al.,[31] Massoli et al.,[32] Vu et al.,[33] and Fofie et al.[34]).

While previous studies have helped highlight the effect of aerosol mixtures on subsaturated hygroscopicity, the knowledge of the effects of LLPS (due to aerosol mixing) on CCN activity has been limited for it is often assumed that the mixed particle fully deliquesces above 100% RH. In a recent paper by Ott et al.,[28] the addition of sucrose on different binary systems that undergo LLPS was investigated through optical microscopy (particles >10 μm). The addition of sucrose shifts the particle morphology from phase-separated to one well-mixed phase (i.e., the LLPS was arrested with a sufficiently large concentration of sucrose). This transition was attributed to the increase in the average O:C ratio, which increased upon the addition of sucrose.[28] Multiple studies have experimentally investigated the effect of the O:C ratio on aerosol water uptake with varying results (Figure 1).[27−29,34−51] Massoli et al.[32] measured the CCN activity of generated secondary organic aerosols (α-pinene, 1,3,5-trimethylbenzene, m-xylene, and 50:50 mixture of α-pinene and m-xylene) of varying O:C ratios (0.3−1) and found that the CCN activity increased as a function of the O:C ratio.[32] Similar correlations have been observed in other studies (including but not limited to Jimenez et al.,[42] Lambe et al.,[44] Wong et al.,[52] and Nakao[41]). Other studies showed little to no direct correlation (including but not limited to Alfarra et al.,[53] Chang et al.,[54] Suda et al.,[55] and Tang et al.[43]). This variability in results indicates that other factors need to be considered to fully represent hygroscopicity. One additional factor reported to be significant for CCN activation is solubility, particularly in the range of 0.1−100 g L^{-1}.[46,47,56] This solubility range was parameterized by Kuwata et al.[51] and corresponds to an O:C range of 0.2−0.7.[41,51]

To date, the relationship between the LLPS, O:C ratio, and solubility is aptly described within the thermodynamic framework of Gibbs free energy. LLPS occurs when the Gibbs free energy of the phase-separated system is less than the Gibbs free energy of the homogeneous, well-mixed system, assuming that the activation barrier is sufficiently low for LLPS to occur.[45,48] Whether a system undergoes LLPS is correlated with its O:C ratio, solubility, and, therefore, water uptake.

https://doi.org/10.1021/acsenvironau.3c00015
ACS Environ. Au 2023, 3, 348−360

Roughly, compounds with more oxygen atoms tend to be more soluble in aqueous solutions and more hygroscopic due to the potential for hydrogen bonding with the solvent and are less likely to undergo LLPS. Compounds with fewer oxygen atoms (e.g., in the extreme, carbonaceous graphitic soot or primary organic aerosol) tend to be less soluble in aqueous solutions and are more likely to undergo LLPS.[57] Note that the exact functional groups and identity of the organic compound are also important in determining whether LLPS occurs.[28] While predicting LLPS from first principles remains a challenge, previous literature has utilized models like AIOMFAC to predict LLPS formation in mixtures (including but not limited to Zuend and Seinfeld,[27] Hodas et al.,[30] and Chang and Pankow[58]). However, if unspeciated organic aerosol exists, as observed in the atmosphere, it becomes increasingly more difficult to predict Gibbs free energy and derived activity coefficients. This is also particularly true for atmospherically relevant systems with more than one organic species (ternary or greater mixtures) where organic−organic interactions in addition to organic−inorganic interactions must also be considered. Additionally, while LLPS has been shown to exist in subsaturated conditions,[59] few studies have reported the impact of LLPS under supersaturated conditions.[13,60] It is often assumed that particles are well mixed and deliquesce above 100% RH. Hence, this study aims to elucidate these factors by investigating the CCN activity of two ternary systems containing sucrose, ammonium sulfate (AS), and one organic compound (2MGA or PEG1000) that undergoes LLPS with AS.[28,61] AS is a major constituent of atmospheric aerosols and a good proxy for inorganic compounds in model mixtures, while sucrose is a good proxy for highly soluble organic compounds with a high O:C ratio (Table S1). Organic 2MGA, a surface-active chemical and one of the most abundant methyl-substituted dicarboxylic acids, is ubiquitous in the troposphere.[61−63] PEG1000 is a polymer and is less atmospherically relevant. However, PEG1000 is also known to undergo LLPS with AS and has a significantly higher solubility than 2MGA (Table S1). The CCN activity of these two different systems (the 2MGA system and the PEG1000 system) was measured at varying compositions using a cloud condensation nuclei counter (CCNC) and compared to that of different theoretical models. To help further enhance our CCN results, optical microscopy images, cryogenic-transmission electron microscopy images, and surface tension measurements were reported. The following results provide insights into the impact of solubility, O:C ratio, and phase transition on measured droplet activations and, as a result, will help improve theoretical CCN predictions of complex mixtures. Furthermore, the results presented may be extended to other humid environments, such as supersaturated conditions found in the respiratory system or humid fog conditions.

2. MATERIALS AND METHODS

2.1. Chemicals

All the chemicals were purchased and used as received without further modification: AS [$(NH_4)_2SO_4$, ≥99%, CAS 7783-20-2, Sigma-Aldrich], 2MGA ($C_6H_{10}O_4$, 98%, CAS 18069-17-5, Sigma-Aldrich), PEG1000 (CAS 25322-68-3, Sigma-Aldrich), and sucrose ($C_{12}H_{22}O_{11}$, 99%, CAS 57-50-1, Fischer Scientific).

2.2. Solution Preparation

Two ternary systems, the 2MGA system (2MGA, AS, and sucrose) and the PEG1000 system (PEG1000, AS, and sucrose), were prepared at different weight percent compositions (Figures S4 and S5). For each system, the three chemicals were weighed individually and poured into a glass media bottle. Approximately 100 mL of ultrapurified water (18 MΩ•cm, Millipore) was added to the chemicals, and the solution was sonicated until all the chemicals were dissolved. In both systems, a wide range of O:C ratios were targeted to include experiments in regions where LLPS is present and where LLPS is not present (Figure S1). The phase transition (the absence/presence of LLPS) for each of the two systems (see the yellow-shaded region in Figure S1) was based on the experimental findings of the Ott et al.[28] paper. In the case of the 2MGA system, Ott et al. reported a halt to LLPS at an O:C ratio of 0.72 and above. As for the PEG1000 system, the LLPS was halted at an O:C ratio of 0.91 and above.[28] It is important to note that Ott et al.[28] conducted the experiments at one ratio of 2MGA/AS (50−50 wt %) and one ratio of PEG1000/AS (50/50 wt %) and the O:C ratio was increased by incremental addition of sucrose. In addition to the Ott et al. paper, the phase diagrams for both AS and 2MGA[45] and AS and PEG1000[48] were also considered to identify where LLPS is observed for both systems. By examining the hygroscopicity of particles from both systems over a wide range of O:C values, we were able to determine how the presence or absence of LLPS affects CCN activity.

2.3. Cloud Condensation Nuclei Measurements

The water uptake of the two ternary systems of different chemical compositions was measured under supersaturated conditions using a CCNC (Droplet Measurement Technologies[64,65]). A detailed experimental setup is provided in Figure S3. In brief, aerosols were generated using a Collison nebulizer (Atomizer; TSI 3076). The wet aerosols generated were then passed through two diffusion dryers to reduce the RH to less than 5% RH (measured using a Vaisala HMP60 probe). The dry polydisperse aerosols were size-selected (8 to 352 nm; 135 s scan time) by a differential mobility analyzer (DMA; TSI 3080). A stream of monodisperse aerosols exits the DMA and is then split into two streams. One stream (0.3 L min^{-1}) enters the condensation particle counter (CPC; TSI 3776)—where the concentration of particles (CN) is measured. The second stream (0.5 L min^{-1}) enters the CCNC—where the concentration of activated particles (CCN) is measured. The scanning mobility CCN analysis (SMCA), a widely used method for CCN analysis in previous literature,[66−69] was used to analyze the data. The SMCA performs a charge-correction procedure and removes artifacts from multiply charged particles.[70] SMCA also calculates the activation ratio $\frac{CCN}{CN}$ at every supersaturation. A sigmoid fit is applied to the activations data to obtain the critical diameter, D_d, the size at which half of the particles are activated. The D_d for each experiment was measured at four different supersaturations (0.41, 0.59, 0.77, and 0.97%) (refer to Figure S2 and Table S2 for CCNC supersaturation calibration). For each experiment, an average D_d and its respective standard deviation were reported at each supersaturation.

2.4. Optical Microscopy

The morphology of particles from the 2MGA system and the PEG1000 system was investigated using an inverted optical microscope with a home-built environmental chamber that enables the phase transition characterization of micrometer particles. A detailed experimental procedure has been described in previous literature.[28,50] In brief, ternary solutions of different compositions (refer to Supporting Information, Section VI) were prepared in HPLC-grade water. Droplets were generated by spraying aqueous solutions onto hydrophobic glass slides. Particles of sizes ranging from 20 to 200 μm in diameter were observed using a Nikon Eclipse Ti2 microscope. The RH was altered by injecting a flow of wet and dry nitrogen into the chamber containing the slide and sample. The RH within the chamber was measured with a ±3% uncertainty using a Vaisala HMP60 probe. After equilibrating the droplets, the RH was decreased at a rate of ∼1% RH min^{-1} until the phase transition was reached, followed by an RH rate decrease to ∼0.5% RH min^{-1} until the phase transition was deemed finished. For each experiment, a minimum of 30 particles were studied.

https://doi.org/10.1021/acsenvironau.3c00015
ACS Environ. Au 2023, 3, 348−360

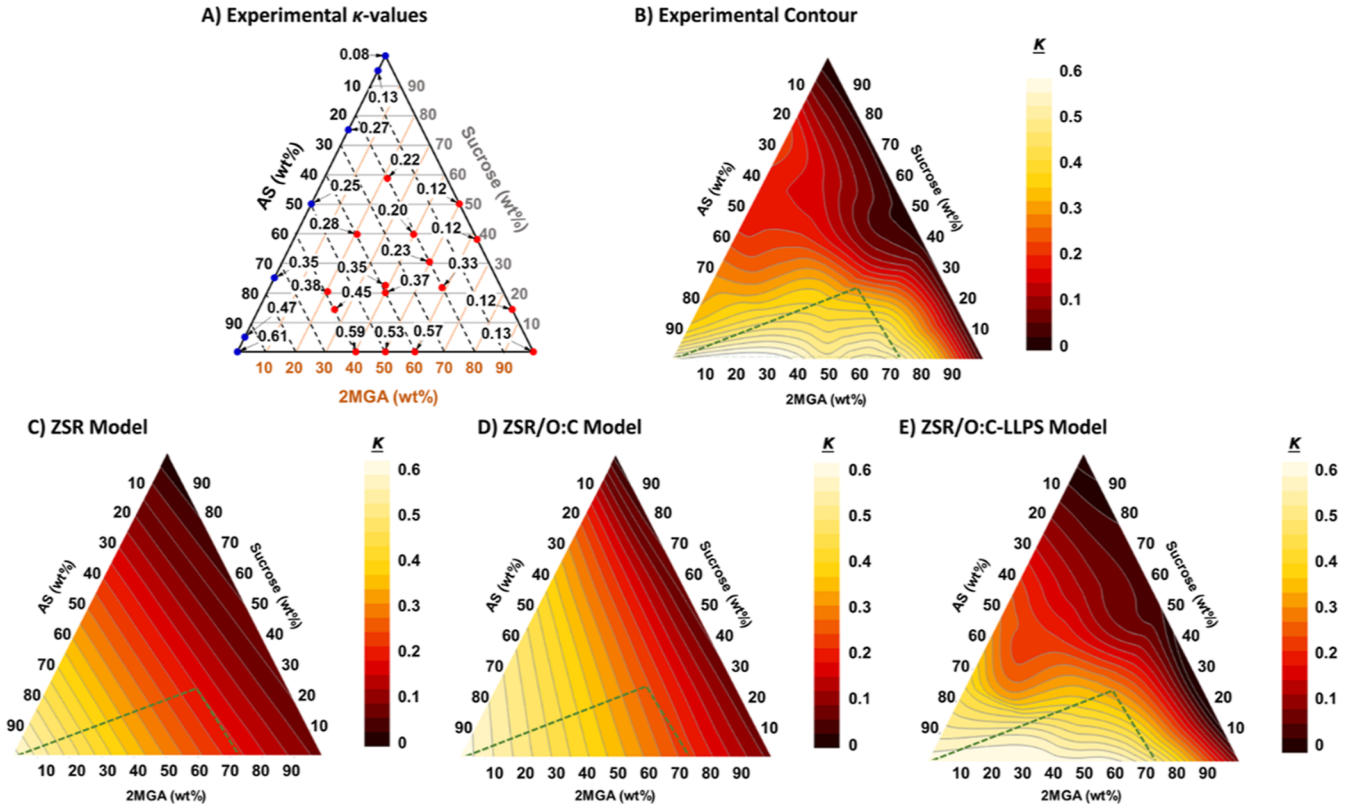

Figure 2. κ-hygroscopicity for the 2MGA system presented in ternary plots (the vertices of the triangles represent 100% pure compounds: bottom left vertex = 100% AS, bottom right vertex = 100% 2MGA, and top vertex = 100% sucrose). (A) Experimental κ-values are determined at the nodes: red circles represent experiments from this work; blue circles represent results obtained from the study by Razafindrambinina et al.,[79] (B) experimental contour plot of κ-values extrapolated from experimental κ-values at the nodes shown in A, (C) ZSR model, (D) ZSR/O:C model, and (E) ZSR/O:C-LLPS model. (B–E) the color gradient shows the range of κ-hygroscopicity values in the ternary system. The region where LLPS is assumed to exist is outlined in the dotted green lines.

3. RESULTS AND DISCUSSION

The water uptake of the 2MGA system and the PEG1000 system was investigated under four supersaturated conditions (0.41, 0.59, 0.77, and 0.97%) using the CCNC. Both systems' water uptake was measured at different chemical compositions, and the average hygroscopicity parameter, κ, of each system is reported in a ternary heat plot. For each system, the results of our experimental κ-hygroscopicity values were evaluated with respect to three different theoretical models, namely, the ZSR model, the ZSR/O:C model, and the ZSR/O:C-LLPS model. These models are each described in Supporting Information, Sections VIII.

3.1. CCN Activity of the 2MGA System

Mixtures of AS, sucrose, and 2MGA of different chemical compositions were prepared and investigated for their water uptake efficiencies under supersaturated conditions. The experimental κ-hygroscopicity value was calculated for each mixture (Figure S4 and Table S3), and the results are presented in a ternary plot (Figure 2A). Figure 2A shows the experimental κ-hygroscopicity values with pure AS occupying the bottom left vertex, pure sucrose occupying the top vertex, and pure 2MGA occupying the bottom right vertex. The experimental κ-values obtained for AS and sucrose are 0.61 ± 0.04 and 0.08 ± 0.02, respectively. The CCN activity of AS and sucrose is widely studied, and our experimental κ-values are consistent with those of previous literature.[71,72] As for the hygroscopicity of pure 2MGA, the experimental κ-value obtained was 0.13 ± 0.02. To our knowledge, no previous literature has reported the experimental water uptake efficiency of pure 2MGA particles under supersaturated conditions. A prior study by Marsh et al.[73] investigated the hygroscopicity, under subsaturated conditions, of 2MGA along with various other carboxylic acids using a comparative kinetics electrodynamic balance. The κ-value for 2MGA was reported to be 0.102 ± 0.005 (RH = 95%), while the κ-values of glutaric acid, 3-methylglutaric acid, 2,2-dimethylglutaric acid, and 3-methyl adipic acid were reported to be 0.144 ± 0.005, 0.103 ± 0.006, 0.116 ± 0.009, and 0.064 ± 0.002, respectively.[73] This study's κ-value of 2MGA (0.13 ± 0.02) is higher than the reported subsaturated κ-value of 2MGA (0.102 ± 0.005) reported by Marsh et al.[73] This higher κ-value can be attributed to the difference in experimental systems; κ-values derived from supersaturated conditions are typically larger than those derived from subsaturated measurement. Various studies have observed higher supersaturation-derived κ-values relative to their respective subsaturated κ-values and attributed this difference to the particle solute solubility or surface tension depression by surface-active organic molecules under supersaturated conditions.[71,72,74−78] Adsorption-driven water uptake mainly pertains to effectively water-insoluble solutes.[77] Also, since 2MGA is the only weakly water-soluble component (>10 g L^{-1}), the surface tension effects of 2MGA are further explored here.

The Köhler model assumes that surface tension is equal to that of pure water (72 mN m^{-1}); however, a surface-active

https://doi.org/10.1021/acsenvironau.3c00015
ACS Environ. Au 2023, 3, 348−360

compound can impact the Kelvin effect by lowering the droplet's effective vapor pressure under supersaturated conditions, which leads to a perceived higher κ-value.[80,81] To measure the magnitude of surface activity, the surface tension of pure 2MGA was measured at different concentrations (0.1−0.7 M) with a pendant drop tensiometer (Figure S11). The results show that 2MGA is surface-active with a surface tension depression of more than ∼25%. A previous paper has reported a surface tension depression of 20% to have an impact on CCN κ-values.[76] Hence, the difference in this study's κ-value of 2MGA and the κ-value reported by Marsh et al.[73] can be justified by the surface tension properties of 2MGA. Surface tension is not the dominant effect for water uptake in the subsaturated regime as the droplet interface is small.[76]

Experimental κ-values from Figure 2A were used to extrapolate κ-values across the ternary plot and are presented as a contour in Figure 2B. The κ-values in the experimental contour plot also vary from 0.08 to 0.61 with respect to chemical composition (Figure 2B). Specifically, in the region where LLPS is predicted to occur (denoted by the area inside the green dotted line), the experimental κ-values are ∼ ≥ 0.4 (Figure 2A,B). This value indicates that AS, and the most hygroscopic compound, is the dominant chemical in the water uptake process in the LLPS region. This trend has been observed in a study conducted by Altaf et al.[13] The study reported that a 50:50 mixture of AS/succinic acid and AS/pimelic acid with a partially engulfed/phase-separated morphology results in CCN activity close to that of AS.[13] As for the region where LLPS is not present, our experimental κ-values were observed to change linearly, indicating that all three chemicals contribute to the water uptake—a trend that agrees with results observed by Altaf et al.[13] The study by Altaf et al. investigated the CCN activity of mixtures of AS/pimelic acid and AS/succinic acid with homogeneous morphology and found the CCN activity to fall between the pure compounds—indicating all components to be involved in the water uptake process.[13] Hence, our experimental results for the 2MGA system indicate that the presence or lack of LLPS plays a key role in droplet growth and CCN activity.

To help explain the experimental κ-values derived from the 2MGA ternary system, we compared our experimental values to the theoretical κ-values obtained from the hygroscopicity ZSR model (Figure 2C). Figure 2C shows that the ZSR κ-values change uniformly with the volume fraction (note that all three axes are in terms of weight %), indicating that all three chemicals contribute equally to the water uptake. Comparing the experimental κ-hygroscopicity results with the ZSR model, which assumes contributions from all solutes based on their molar volumes, visible discrepancies between the experimental results and the ZSR model exist. Specifically, the experimental κ-values around the LLPS region are observed to deviate from the linearity found in the ZSR model within the same region. A regression plot was generated to help quantitatively evaluate the ZSR model to our experimental results (Figure 3). The regression plot shows a poor correlation with an R^2 value of 0.65. Specifically, less agreement between the experimental and predicted κ-values is observed when the κ-values are >0.4. This divergence between our experimental results and the ZSR model once again suggests that LLPS might play a role in the water uptake process.

Since the presence/absence of LLPS is correlated with the O:C ratio, as seen in previous literature (Massoli et al.,[32] Ott et al.,[28] Song et al.,[45] and You et al.[57] to name a few), a

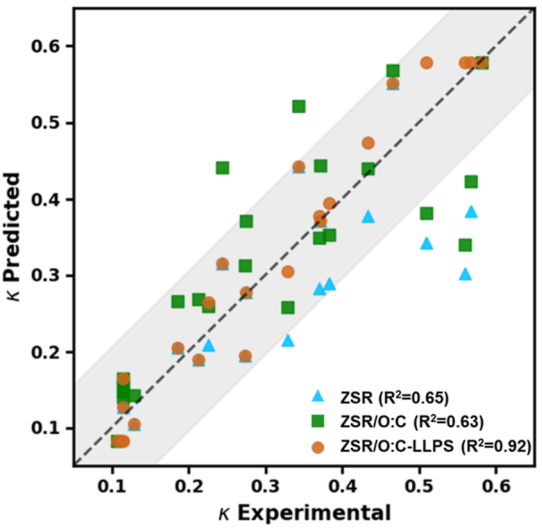

Figure 3. 2MGA system's κ-experimental versus κ-predicted values obtained from the ZSR hygroscopicity model (light blue triangles), the ZSR/O:C hygroscopicity model (green squares), and the ZSR/O:C-LLPS hygroscopicity model (brown circles). The black dotted line is the 1:1 ratio line; the gray region shows a 95% prediction interval across the 1:1 line.

theoretical model that integrates the O:C ratio into the hygroscopicity ZSR model, namely, the hygroscopicity ZSR/O:C model was employed. The hygroscopicity ZSR/O:C model estimates κ-hygroscopicity based on the solubility of the mixture as estimated with the O:C ratio. The solubility of a mixture was parameterized through the average O:C ratio as reported by Nakao.[41] Like the ZSR model, the ZSR/O:C model shows poor agreement with our experimental data (Figures 2D and 3). The ZSR/O:C model also exhibits a linear gradient of κ-values that is comparable to that of the ZSR model but differs in the amounts that each chemical contributes to the water uptake processes. In the ZSR/O:C model, high κ-values (>0.4) occupy ∼50% of the ternary plot, compared to only ∼30% in the ZSR model. This difference indicates that AS has a stronger contribution to the water uptake process in the ZSR/O:C model. Considering that the solubility of each chemical is accounted for within the model, AS having a strong contribution can be attributed to the high solubility of AS relative to glucose and 2MGA. When comparing the ZSR/O:C hygroscopicity model to the experimental results, it is evident that the ZSR/O:C model itself does not help explain the κ-values obtained from experimental results. This difference is further highlighted by the poor correlation between the two models, with an R^2 value of 0.63 obtained from the regression plot in Figure 3. However, a visible similarity is observed within the LLPS region for both our experimental results and the ZSR/O:C model. The ZSR/O:C model results in high κ-values (>∼0.3) within the LLPS region, which indicates that CCN activity is strongly influenced by AS; a trend that agrees with our experimental data.

Despite the fact that the two aforementioned models do not accurately describe our results, our experimental results show resemblance with the ZSR model above the LLPS region and some resemblance with the ZSR/O:C model below the LLPS region. Thus, a third model, namely, the ZSR/O:C-LLPS hygroscopicity model that accounts for LLPS was also explored. The ZSR/O:C-LLPS model is shown in Figure 2E. The ZSR/O:C-LLPS model assumes that the 2MGA is not

https://doi.org/10.1021/acsenvironau.3c00015
ACS Environ. Au 2023, 3, 348−360

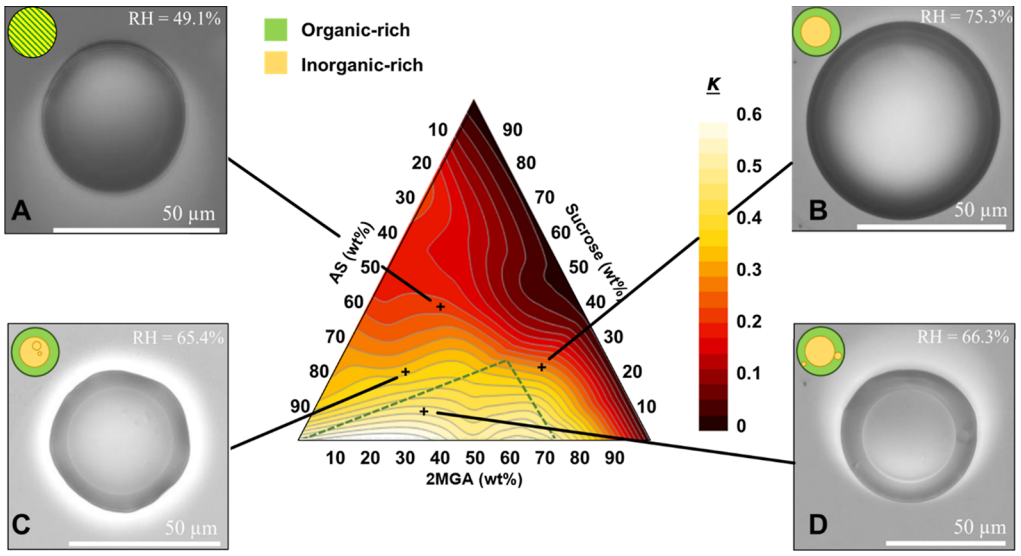

Figure 4. Optical microscopy images and illustrations of particles obtained from four different regions in the 2MGA ternary plot (for experimental details, refer to Figure S5 and Table S4 in the Supporting Information). Image A was taken from a mixture of AS (39.7 wt %) + 2MGA (20.6 wt %) + sucrose (39.7 wt %); image B was taken from a mixture of AS (20.0 wt %) + 2MGA (58.3 wt %) + sucrose (21.7 wt %); image C was taken from a mixture of AS (59.3 wt %) + 2MGA (20.4 wt %) + sucrose (20.3 wt %); and image D was taken from a mixture of AS (60.0 wt %) + 2MGA (31.4 wt %) + sucrose (8.6 wt %). The region where LLPS is assumed to exist is outlined in the dotted green line. The RH at which the images are recorded is shown within each image. The size of all the particles shown is approximately 50 μm.

part of the aqueous phase (the phase responsible for the water uptake) below a specific O:C ratio threshold defined via bootstrapping. While above that specific O:C ratio threshold, the water uptake is driven by all three solutes, and their water uptake contribution is based on their molar volumes. The model, through the bootstrapping method, estimated the threshold O:C ratio to be 0.75 (i.e., LLPS is present when the O:C ratio <0.75 and LLPS is not present when the O:C ratio >0.75). This predicted O:C ratio threshold is close to the experimentally attained O:C ratio of 0.72 from the work of Ott et al.[28] Additionally, the theoretical hygroscopicity obtained from the ZSR/O:C-LLPS model (Figure 2E) shows a strong resemblance to our experimental hygroscopicity results (Figures 2B and 3). To quantitatively evaluate this model to our experimental results, a regression plot was produced (Figure 3), showing that all the experimental κ-values fall within the 95% confidence interval of the κ-values generated by the ZSR/O:C-LLPS model. Additionally, the ZSR/O:C-LLPS hygroscopicity model agrees well with experimental κ-values >0.3, whereas the previous models did not. The R^2 value of 0.92 shows a strong agreement between our experimental results and the ZSR/O:C-LLPS model, indicating that this model is the best model for predicting the 2MGA system's ternary hygroscopicity. The strong agreement between our experimental results and the ZSR/O:C-LLPS model provides insights into the water uptake process of the ternary system. It implies that below the theoretically predicted O:C ratio of 0.75, 2MGA is not part of the aqueous phase and is not contributing to the water uptake, while at an O:C ratio >0.75, all three components are involved in the water uptake process. The absence of 2MGA in the aqueous phase (O:C ratio <0.75) can be attributed to the poor water-solubility of 2MGA (40.6 g L^{-1}) relative to AS (74.4 g/100 g) and sucrose (824 g L^{-1}).

To further our understanding of this system, optical microscopy images of particles were obtained at different regions within the ternary plot (Figure 4). The four experiments that were performed to obtain microscale images of particles were chosen to cover regions that have LLPS and regions that do not have LLPS (Figure S6 and Table S5). Figure 4A represents the morphology of a particle from a mixture with an O:C ratio of 0.78. The image indicates that there is no phase separation present, which is expected since it is outside the LLPS region. Hence, the water uptake activity depends on AS, sucrose, and 2MGA with respect to their molar volumes. Figure 4B represents a particle obtained from a mixture with an O:C ratio of 0.70. The particle consists of a phase-separated morphology. The separation RH (SRH) was 65.2 ± 9.9 % RH. The Ott et al.[28] paper reported the SRH for a 50−50 wt % mixture of AS and 2MGA to be 79.4 ± 1.0 % RH, and the addition of sucrose leads to lower values of the SRH. Hence, the particle in Figure 4B has a lower SRH likely due to the influence of sucrose. Figure 4C shows an image of a particle obtained from a mixture with an O:C ratio of 0.74. The particle consists of a phase-separated morphology but also contains inorganic-rich inclusions. The SRH for this particle was found to be 63.9 ± 4.7 % RH. A similar trend is also seen in the particle (O:C = 0.69) provided in Figure 4D. The particle has an SRH of 72.4 ± 2.2 % RH. Note that the experimental O:C ratio value of 0.72 (obtained from the study by Ott et al.[28]) as the region for phase separation is an estimate based on one 2MGA-to-AS ratio and that this value may vary slightly as a function of the composition of 2MGA, AS, and sucrose. The presence of inclusions may indicate that the phase separation process has not reached the thermodynamic equilibrium,[45,49] which may result in different compositions in the inorganic-rich and organic-rich phases than at equilibrium. However, inclusions are expected to be less likely in submicron particles as these systems reach equilibrium more rapidly.[45,82] It is also important to note that the experimental examination of morphology for the 2MGA system above has focused on droplets 20−200 μm in diameter, and morphology can be different for submicron aerosol particles. Specifically, phase separation can be inhibited in sufficiently small aerosol

https://doi.org/10.1021/acsenvironau.3c00015
ACS Environ. Au 2023, 3, 348−360

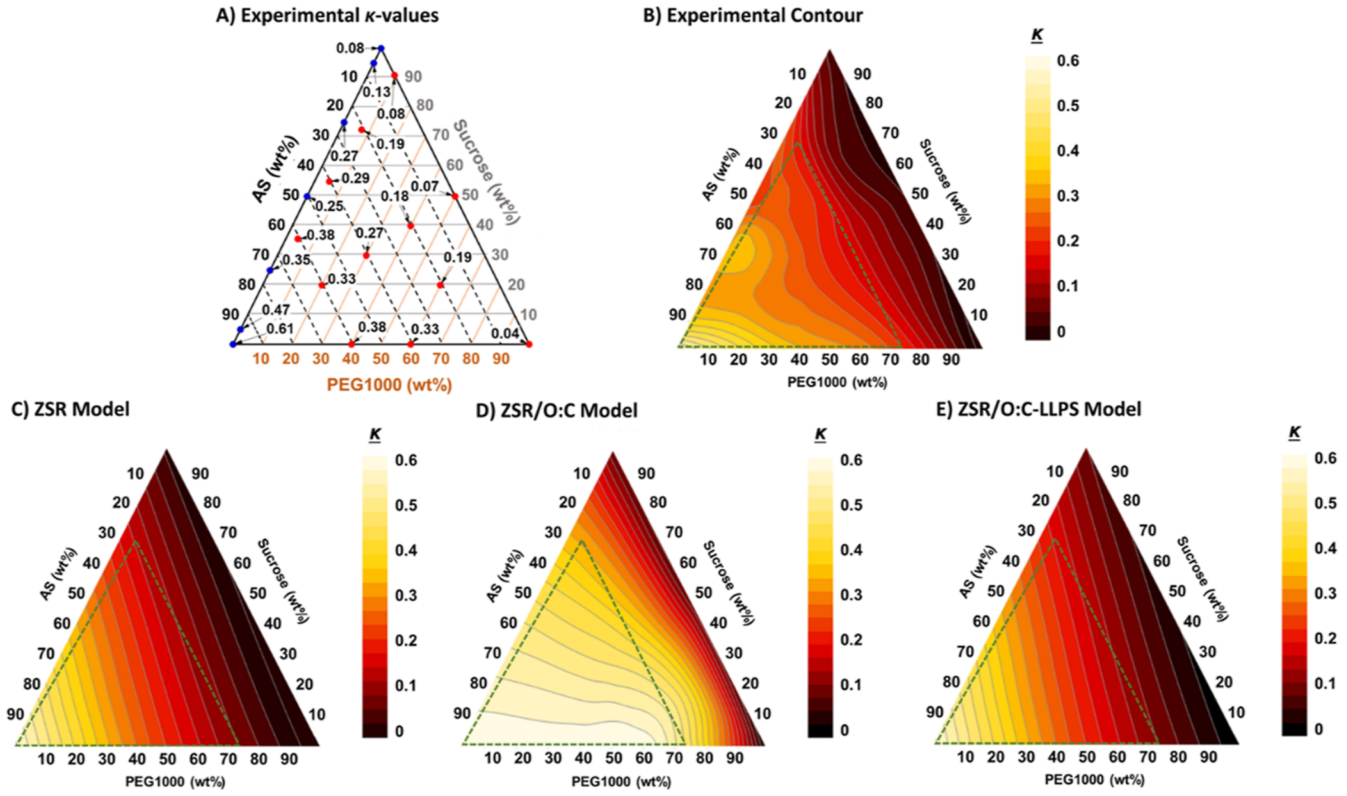

Figure 5. The κ-hygroscopicity for the PEG1000 system presented in ternary plots (the vertices of the triangles represent 100% pure compounds: bottom left vertex = 100% AS, bottom right vertex = 100% PEG1000, and top vertex = 100% sucrose). (A) Experimental κ-values are determined at the nodes: red circles represent experiments from this work; blue circles represent results obtained from the study by Razafindrambinina et al,[79] (B) experimental contour plot of κ-values extrapolated from experimental κ-values at nodes shown in (A), (C) ZSR model, (D) ZSR/O:C model, and (E) ZSR/O:C-LLPS model. (B–E) the color gradient shows the range of κ-hygroscopicity values in the ternary system. The region where LLPS is assumed to exist is outlined in the dotted green lines.

particles, which may affect CCN measurements.[26] A discussion is provided in Supporting Information, Section VII.

3.2. CCN Activity of the PEG1000 System

The hygroscopicity of the PEG1000 ternary system was also investigated under supersaturated conditions. The experimental κ-hygroscopicity was averaged across four different supersaturations for each mixture (Figure S5 and Table S4) and mapped using a ternary plot (Figure 5A). Figure 5A shows the experimental κ-hygroscopicity values in a ternary heat plot with pure AS occupying the bottom left vertex, pure sucrose occupying the top vertex, and pure PEG1000 occupying the bottom right vertex. The experimental κ-values obtained for AS and sucrose are as reported above in the results of the 2MGA system. As for PEG1000, the experimental κ-value obtained was 0.04 ± 0.02. Hodas et al.[83] investigated the CCN activity of PEG1000 under 0.8% supersaturation and reported the κ-value to be 0.07; no uncertainty value was reported. The discrepancy between our experimental κ-value and the κ-value obtained by Hodas et al.,[83] may be attributed to the difference in proportions of PEG1000 with varying chain lengths in the sample. The length of the carbon chain has been shown to impact the hygroscopicity of organic aerosols. Petters et al.[84] reported that the hygroscopicity of hydroperoxyacids and dihydroperoxides decreased with increasing carbon chain length. Additionally, variability in polymer chain lengths would lead to change in molecular weight—a property that has been reported to impact aerosol hygroscopicity.[37,85,86]

κ-values derived from experimental data are shown in Figure 5A,B shows a contour plot of κ-values extrapolated from experimental κ-values derived in Figure 5A. It is also evident that mixtures of AS, sucrose, and PEG1000 at various weight percent compositions result in different κ-values ranging between 0.04 and 0.61. Like the 2MGA system, to analyze the experimental κ-values obtained from the PEG1000 system, we first compared our experimental results to the simplest theoretical κ-values obtained from the ZSR hygroscopicity model (Figure 5C). Figure 5C shows a ternary plot representing the theoretical κ-values of mixtures containing AS, sucrose, and PEG1000 at different chemical compositions. The uniformity in κ-values shown in Figure 5C indicates that the water uptake of a mixture is linearly additive—all three chemicals contribute to the water uptake ZSR model. A graphical resemblance is observed between the ZSR model (Figure 5C) and our experimental results (Figure 5B). A regression plot, provided in Figure 6, shows that there is a good correlation between our experimental results and the ZSR model (R^2 = 0.84), with only one data point falling outside the 95% confidence region. This indicates that the hygroscopicity of the PEG1000 system can be aptly modeled by the ZSR model. However, to investigate the potential effect of the O:C ratio and LLPS, the ZSR/O:C model and the ZSR/O:C-LLPS model were generated as well.

The ZSR/O:C hygroscopicity model (shown in Figure 5D) was developed to explore the effect of the O:C ratio on the PEG1000 system. The κ-values for the PEG1000 system generated through the ZSR/O:C model indicate that AS is the

https://doi.org/10.1021/acsenvironau.3c00015
ACS Environ. Au 2023, 3, 348−360

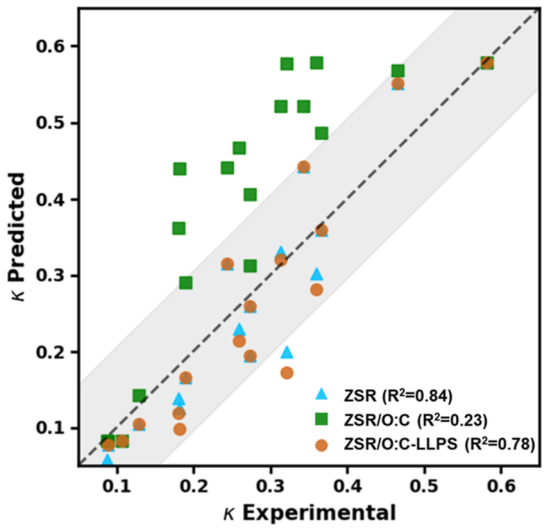

Figure 6. PEG1000 system's κ-experimental versus κ-predicted values obtained from the ZSR hygroscopicity model (light blue triangles), the ZSR/O:C hygroscopicity model (green squares), and the ZSR/O:C-LLPS hygroscopicity model (brown circles). The black dotted line is the 1:1 ratio line; the grey region shows a 95% prediction interval across the 1:1 line.

dominant force in the water uptake process. This is highlighted by κ-values of $\geq$0.5 in ~90% of the ternary region—a hygroscopicity pattern that does not match experimental results (Figures 5B and 6). This poor correlation is further emphasized by the R^2 value of 0.23 obtained from the regression plot in Figure 6. The ZSR/O:C-LLPS model was also explored, and the generated heat map is presented in Figure 5E. The O:C ratio threshold defined by the bootstrap algorithm was 0.85—an O:C ratio lower than the O:C ratio of 0.91 reported from the experimental results of Ott et al.[28] The hygroscopicity heat map generated by the ZSR/O:C-LLPS hygroscopicity model shows a resemblance to the experimental heat map and to the ZSR model. The regression plot of the ZSR/O:C-LLPS model versus experimental κ-values shows a strong correlation with only one data point not within the 95% confidence region. The R^2 value associated with this regression plot was 0.78 and indicates that the ZSR/O:C-LLPS model is better at estimating the PEG1000 system than the ZSR/O:C model (R^2 = 0.23) but not as good as the ZSR model (R^2 = 0.84). Both the ZSR model (R^2 = 0.84) and the ZSR/O:C-LLPS model (R^2 = 0.78) may be used to predict the hygroscopicity of the PEG1000 system. From Figure 6, the ZSR model and the ZSR/O:C-LLPS model only had one data point that was outside the 95% confidence region. While both models show strong correlation with experimental results, using the ZSR/O:C-LLPS model will not only provide theoretical κ-values; it can also estimate an O:C threshold where LLPS might be present.

The agreement between the ZSR model and the ZSR/O:C-LLPS with experimental results indicates that the O:C ratio does not play a role in CCN activity in the PEG1000 system. This agreement is consistent with the water uptake of polymers that are known to be driven by water interaction parameters and not molar volume solubility alone.[87,88] Subsequently, despite the PEG1000 system being primarily in a LLPS form, experimental data shows that LLPS has no effect on mixed water uptake. This can be attributed to the high solubility and water interaction parameter of PEG1000, and as a result, PEG1000 is integrated into the aqueous phase with AS and sucrose regardless of the presence of LLPS. To help elucidate these results, we examined the morphology of particles.

Optical microscopy was used to explore the morphology of particles in the ternary phase diagram (Figure 7). Experiments were conducted at different regions within the ternary plot to help explain the CCN activity results (Figure S7 and Table S6). The particle presented in Figure 7A is representative of those obtained from a solution with an O:C ratio of 0.91. The

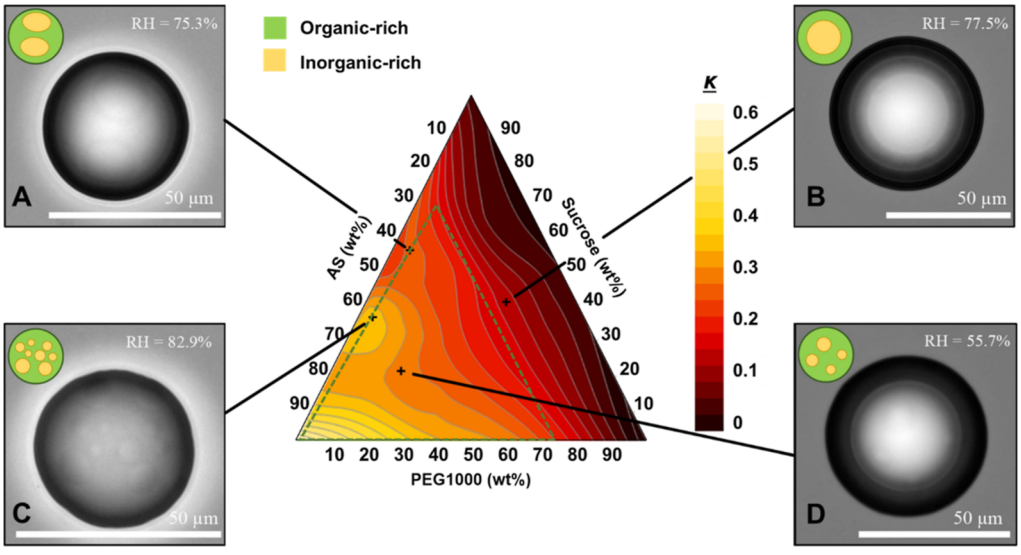

Figure 7. Optical microscopy images and illustration of particles obtained from four different regions in the PEG1000 ternary plot (for experimental details refer to Figure S6 and Table S5 in the Supporting Information). Image A was taken from a mixture of AS (40.0 wt %) + PEG1000 (5.0 wt %) + sucrose (55.0 wt %); image B was taken from a mixture of AS (20.0 wt %) + PEG1000 (40.0 wt %) + sucrose (40.0 wt %); image C was taken from a mixture of AS (60.0 wt %) + PEG1000 (4.1 wt %) + sucrose (35.6 wt %); and image D was taken from a mixture of AS (60.0 wt %) + PEG1000 (20.0 wt %) + sucrose (20.0 wt %). The region where LLPS is assumed to exist is outlined in the dotted green line. The RH at which the images are recorded is shown within the images. The size of the particles shown is ~50 μm.

https://doi.org/10.1021/acsenvironau.3c00015
ACS Environ. Au 2023, 3, 348−360

SRH of particles produced from this composition is 81.6 ± 2.6%. The morphology of the particle indicates that there are two larger inorganic-rich inclusions within the droplet. These inclusions can also be seen in the particles shown in Figure 7C,D but vary in number and size. In particular, the particle in Figure 7C has many smaller inclusions compared with Figure 7A. The inclusions seen in Figure 7A,C,D indicate that the particle is not in its final equilibrium state, which may be related to the viscosity of this system.[28] As a result, the composition of the organic-rich and inorganic-rich phases may differ from the equilibrium compositions, which could affect water uptake, leading to the high κ-values observed. The particle in Figure 7B has a phase-separated morphology although it is slightly outside the region where we predict LLPS to occur. As stated above, this region is an estimate based on one composition of PEG1000 and AS and may differ as this composition is varied. Note also that as discussed for the 2MGA system, the submicron morphology can differ from the supermicron morphology (more details in Supporting Information, Section VII).

4. SUMMARY AND CONCLUSIONS

The aerosol mixtures of different chemical compositions have the ability to impact aerosol physical properties and subsequent hygroscopicity. This study investigates the water uptake of two ternary systems, namely, the 2MGA system (AS + sucrose + 2MGA) and the PEG1000 system (AS + sucrose + PEG1000) that undergo LLPS as the O:C ratio is modified in the aerosol. The mixtures are indicative of exemplary aerosol sources (including but not limited to atmospheric, pharmaceutical, ambient indoor, and combustion) that contain complex organic materials. To our knowledge, no previous study has examined the ternary effect of LLPS on the κ-hygroscopicity and droplet growth of internal aerosol mixtures. Several previous studies have investigated binary aerosol mixtures, and because it is assumed that full deliquescence occurs above 100% RH, few studies have explored LLPS ternary systems with CCN activation. Thus, the results here advance our overall understanding of the impact of phase transitions on water uptake in a wide range of environments. Furthermore, the results here highlight that organic−organic interactions must be considered in addition to inorganic−organic interactions. For each ternary system, hygroscopicity experiments on different chemical compositions were conducted using a CCNC at four different supersaturations (0.41, 0.59, 0.77, and 0.97%). The κ-hygroscopicity values of the 2MGA system and the PEG1000 system were presented and compared to single theoretical models. Our results indicate that for mixtures that do not undergo LLPS, the κ-hygroscopicity is linearly additive with volume fractions—all chemicals are involved in the water uptake process based on their volume ratio. Hence, the κ-hygroscopicity of well-mixed aerosol can be predicted using the simple ZSR-based hygroscopicity model for both the 2MGA system and the PEG1000 system. However, for mixtures that undergo LLPS, the hygroscopicity prediction is not as straightforward. For the 2MGA system, the LLPS that occurs at an O:C ratio <0.72−0.75 needs to be accounted for when predicting κ-hygroscopicity. The experimental κ-values obtained within the LLPS region show that the three chemicals do not contribute equally to the water uptake process. Instead, the results show that 2MGA has only a negligible contribution to the water uptake process, and this can be attributed to the solubility limits of 2MGA. The solubility of 2MGA is less than that of sucrose and AS, and as a result, 2MGA precipitates and is likely not part of the aqueous phase that contributes to water uptake. As for the PEG1000 system, the experimental κ-values obtained within the LLPS region (O:C ratio <0.85−0.91) show that all three chemicals contribute to the water uptake process. Hence, the LLPS within PEG1000 mixtures show a weak impact on hygroscopicity. This result is attributed to PEG1000's higher solubility compared to that of AS and sucrose. The results of this work offer experimental evidence, analytical insights, and a paradigm shift with regard to the contribution of LLPS to supersaturated droplet activation. Hence, this study highlights the importance of accounting for the LLPS in mixtures. Solubility is not the only factor that contributes to aerosol miscibility. The hygroscopicity of aerosol mixtures that fall within the LLPS region varies substantially based on the morphology, and the region can now be approximated experimentally and theoretically. Mixtures that fall above the LLPS region are likely to be well mixed in the aqueous phase and, as a result, behave with ideal Raoult's law and ZSR hygroscopicity assumptions. This work is the first to experimentally link and propose a method to relate O:C composition, solubility, morphology, and hygroscopicity and thus can be incorporated into droplet models and regional cloud predictions of unspeciated inorganic−organic mixtures. The experimental droplet activation approach to define the relationship between LLPS, O:C, and solubility aligns with previously defined LLPS from water activity coefficients defined with AIOMFAC simulations because hygroscopicity and droplet activities are also functions of water activity. It should be noted that our study explores the CCN activation of dry mixed particles and thus the activation of wet particles exposed to an equilibrium RH above that of LLPS mixing may be different. That is, well-mixed wet particles, when activated into droplets, are unlikely to exhibit LLPS-like effects during activation. Thus, the consideration of thermodynamics and the kinetics of activation in the exhibition of LLPS needs to be explored. Future work should also tackle the role of surfactants in CCN activity. In our study, both 2MGA and PEG1000 were shown to have similar surface tension properties; hence, the difference in the observed results between the two systems cannot be solely attributed to surface tension. Additionally, this study parameterized solubility through the O:C ratio of the mixture; however, this parameterization may not be robust for nitrogen-containing organic species. The O:C ratio is a useful parameter because it is readily measured in ambient studies when the chemical speciation of the organic aerosol is unknown, and in future work, it may be translated to predict droplet growth. In this work, the theoretical ZSR/O:C-LLPS hygroscopicity model that accounts for LLPS through the O:C ratio can predict the hygroscopicity of internally mixed water-soluble systems of different chemical compositions. Thus, this work provides important contributions to link aerosol chemical composition, air quality, hygroscopic growth, and aerosol−cloud climate interactions.

■ ASSOCIATED CONTENT

Supporting Information

The Supporting Information is available free of charge at https://pubs.acs.org/doi/10.1021/acsenvironau.3c00015.

Additional details on chemicals and methods (PDF)

https://doi.org/10.1021/acsenvironau.3c00015
ACS Environ. Au 2023, 3, 348−360

AUTHOR INFORMATION

Corresponding Authors

Timothy M. Raymond − *Department of Chemical Engineering, Bucknell University, Lewisburg, Pennsylvania 17837, United States*; Email: traymond@bucknell.edu

Dabrina D Dutcher − *Department of Chemical Engineering and Department of Chemistry, Bucknell University, Lewisburg, Pennsylvania 17837, United States*; Email: ddd014@bucknell.edu

Miriam Arak Freedman − *Department of Chemistry and Department of Meteorology and Atmospheric Science, Pennsylvania State University, University Park, Pennsylvania 16802, United States*; orcid.org/0000-0003-4374-6518; Email: maf43@psu.edu

Akua Asa-Awuku − *Department of Chemical and Biomolecular Engineering and Department of Chemistry and Biochemistry, University of Maryland, College Park, Maryland 20742, United States*; orcid.org/0000-0002-0354-8368; Email: asaawuku@umd.edu

Authors

Kotiba Malek − *Department of Chemical and Biomolecular Engineering, University of Maryland, College Park, Maryland 20742, United States*

Kanishk Gohil − *Department of Chemical and Biomolecular Engineering, University of Maryland, College Park, Maryland 20742, United States*

Esther A. Olonimoyo − *Department of Chemistry and Biochemistry, University of Maryland, College Park, Maryland 20742, United States*

Nahin Ferdousi-Rokib − *Department of Chemical and Biomolecular Engineering, University of Maryland, College Park, Maryland 20742, United States*

Qishen Huang − *Department of Chemistry, Pennsylvania State University, University Park, Pennsylvania 16802, United States*

Kiran R. Pitta − *Department of Chemistry, Pennsylvania State University, University Park, Pennsylvania 16802, United States*

Lucy Nandy − *Department of Chemistry, Pennsylvania State University, University Park, Pennsylvania 16802, United States*; orcid.org/0000-0001-7647-9837

Katelyn A. Voss − *Department of Chemistry, Pennsylvania State University, University Park, Pennsylvania 16802, United States*

Complete contact information is available at: https://pubs.acs.org/10.1021/acsenvironau.3c00015

Author Contributions

K.M. designed, collected, and analyzed CCN experimental data. K.G. produced and analyzed theoretical models. E.A.O. conducted surface tension measurements. Q.H., K.R.P., L.N., and K.V. designed, collected, and analyzed optical microscopy experiments. Q.H. and K.R.P. designed, collected, and analyzed the electron microscopy experiments. All authors contributed to the writing and preparation of the manuscript. CRediT: **Kotiba Malek** conceptualization (supporting), data curation (lead), formal analysis (lead), investigation (lead), methodology (lead), visualization (equal), writing-original draft (lead), writing-review & editing (lead); **Kanishk Gohil** formal analysis (equal), visualization (equal); **Esther A. Olonimoyo** data curation (supporting), investigation (supporting); **Nahin Ferdousi-Rokib** methodology (supporting), writing-original draft (supporting), writing-review & editing (supporting); **Qishen Huang** data curation (supporting); **Kiran Reddy Pitta** data curation (supporting); **Lucy Nandy** data curation (supporting); **Katelyn A. Voss** data curation (supporting); **Timothy M. Raymond** funding acquisition (equal), project administration (supporting), writing-review & editing (supporting); **Dabrina D Dutcher** funding acquisition (equal), project administration (supporting), writing-review & editing (supporting); **Miriam Arak Freedman** conceptualization (lead), funding acquisition (equal), project administration (equal), supervision (lead), writing-original draft (supporting), writing-review & editing (supporting); **Akua Asa-Awuku** conceptualization (lead), funding acquisition (equal), project administration (equal), supervision (lead), visualization (supporting), writing-original draft (supporting), writing-review & editing (supporting).

Notes

The authors declare no competing financial interest.

ACKNOWLEDGMENTS

K.M., K.G., E.A.O., N.F.-R. and A.A.A. acknowledge support from the NSF: AGS-2124489. Q.H., K.R.P., L.N., K.A.V, and M.A.F. acknowledge support from the NSF: AGS-2124490. D.D.D. and T.M.R. acknowledge support from the NSF: AGS-2124491.

REFERENCES

(1) Seinfeld, J. H.; Pandis, S. N. Atmospheric Chemistry and Physics, 2nd ed., John Wiley & Sons, Inc., 2006, pp 139−152, https://download.e-bookshelf.de/download/0000/7532/93/L-G-0000753293-0002366430.pdf.

(2) The Intergovernmental Panel on Climate Change. *The Physical Science Basis. Contribution of Working Group I to the Fourth Assessment Report of the Intergovernmental Panel on Climate Change*; Cambridge University Press: Cambridge, United Kingdom and New York, NY, USA, 2007; Vol. *996*, pp 113−119.

(3) Ervens, B.; Turpin, B. J.; Weber, R. J. Secondary Organic Aerosol Formation in Cloud Droplets and Aqueous Particles (AqSOA): A Review of Laboratory, Field and Model Studies. *Atmos. Chem. Phys.* **2011**, *11*, 11069−11102.

(4) Manisalidis, I.; Stavropoulou, E.; Stavropoulos, A.; Bezirtzoglou, E. Environmental and Health Impacts of Air Pollution: A Review. *Front. Public Health* **2020**, *8*, 14.

(5) Pöschl, U. Atmospheric Aerosols: Composition, Transformation, Climate and Health Effects. *Angew. Chem., Int. Ed.* **2005**, *44*, 7520−7540.

(6) Oh, H.-J.; Ma, Y.; Kim, J. Human Inhalation Exposure to Aerosol and Health Effect: Aerosol Monitoring and Modelling Regional Deposited Doses. *Int. J. Environ. Res. Public Health* **2020**, *17*, 1923.

(7) Shi, L.; Zanobetti, A.; Kloog, I.; Coull, B. A.; Koutrakis, P.; Melly, S. J.; Schwartz, J. D. Low-Concentration PM2. 5 and Mortality: Estimating Acute and Chronic Effects in a Population-Based Study. *Environ. Health Perspect.* **2016**, *124*, 46−52.

(8) Atkinson, R. W.; Kang, S.; Anderson, H. R.; Mills, I. C.; Walton, H. A. Epidemiological Time Series Studies of PM2. 5 and Daily Mortality and Hospital Admissions: A Systematic Review and Meta-Analysis. *Thorax* **2014**, *69*, 660−665.

(9) Zhang, X. Y.; Wang, Y. Q.; Niu, T.; Zhang, X. C.; Gong, S. L.; Zhang, Y. M.; Sun, J. Y. Atmospheric Aerosol Compositions in China: Spatial/Temporal Variability, Chemical Signature, Regional Haze Distribution and Comparisons with Global Aerosols. *Atmos. Chem. Phys.* **2012**, *12*, 779−799.

(10) Park, R. J.; Jacob, D. J.; Kumar, N.; Yantosca, R. M. Regional Visibility Statistics in the United States: Natural and Transboundary

Pollution Influences, and Implications for the Regional Haze Rule. *Atmos. Environ.* **2006**, *40*, 5405−5423.
(11) Lohmann, U.; Feichter, J. Global Indirect Aerosol Effects: A Review. *Atmos. Chem. Phys.* **2005**, *5*, 715−737.
(12) Wallace, J. M.; Hobbs, P. v. *Atmospheric Science: An Introductory Survey*; Elsevier, 2006; Vol. *92*.
(13) Altaf, M. B.; Dutcher, D. D.; Raymond, T. M.; Freedman, M. A. Effect of Particle Morphology on Cloud Condensation Nuclei Activity. *ACS Earth Space Chem.* **2018**, *2*, 634−639.
(14) Song, M.; Marcolli, C.; Krieger, U. K.; Zuend, A.; Peter, T. Liquid-liquid Phase Separation in Aerosol Particles: Dependence on O: C, Organic Functionalities, and Compositional Complexity. *Geophys. Res. Lett.* **2012**, *39*, DOI: 10.1029/2012gl052807,
(15) Martin, S. T. Phase Transitions of Aqueous Atmospheric Particles. *Chem. Rev.* **2000**, *100*, 3403−3454.
(16) Haywood, J.; Boucher, O. Estimates of the Direct and Indirect Radiative Forcing Due to Tropospheric Aerosols: A Review. *Rev. Geophys.* **2000**, *38*, 513−543.
(17) Marcolli, C.; Luo, B. P.; Peter, T.; Wienhold, F. G. Internal Mixing of the Organic Aerosol by Gas Phase Diffusion of Semivolatile Organic Compounds. *Atmos. Chem. Phys.* **2004**, *4*, 2593−2599.
(18) Song, M.; Marcolli, C.; Krieger, U. K.; Lienhard, D. M.; Peter, T. Morphologies of Mixed Organic/Inorganic/Aqueous Aerosol Droplets. *Faraday Discuss.* **2013**, *165*, 289−316.
(19) Hallquist, M.; Wenger, J. C.; Baltensperger, U.; Rudich, Y.; Simpson, D.; Claeys, M.; Dommen, J.; Donahue, N. M.; George, C.; Goldstein, A. H.; et al. The Formation, Properties and Impact of Secondary Organic Aerosol: Current and Emerging Issues. *Atmos. Chem. Phys.* **2009**, *9*, 5155−5236.
(20) Seinfeld, J. H.; Pankow, J. F. Organic Atmospheric Particulate Material. *Annu. Rev. Phys. Chem.* **2003**, *54*, 121−140.
(21) Bertram, A. K.; Martin, S. T.; Hanna, S. J.; Smith, M. L.; Bodsworth, A.; Chen, Q.; Kuwata, M.; Liu, A.; You, Y.; Zorn, S. R. Predicting the relative humidities of liquid-liquid phase separation, efflorescence, and deliquescence of mixed particles of ammonium sulfate, organic material, and water using the organic-to-sulfate mass ratio of the particle and the oxygen-to-carbon elemental ratio of the organic component. *Atmos. Chem. Phys.* **2011**, *11*, 10995−11006.
(22) Koop, T.; Bookhold, J.; Shiraiwa, M.; Pöschl, U. Glass Transition and Phase State of Organic Compounds: Dependency on Molecular Properties and Implications for Secondary Organic Aerosols in the Atmosphere. *Phys. Chem. Chem. Phys.* **2011**, *13*, 19238−19255.
(23) Pankow, J. F. Gas/Particle Partitioning of Neutral and Ionizing Compounds to Single and Multi-Phase Aerosol Particles. 1. Unified Modeling Framework. *Atmos. Environ.* **2003**, *37*, 3323−3333.
(24) Ciobanu, V. G.; Marcolli, C.; Krieger, U. K.; Weers, U.; Peter, T. Liquid− Liquid Phase Separation in Mixed Organic/Inorganic Aerosol Particles. *J. Phys. Chem. A* **2009**, *113*, 10966−10978.
(25) Marcolli, C.; Krieger, U. K. Phase Changes during Hygroscopic Cycles of Mixed Organic/Inorganic Model Systems of Tropospheric Aerosols. *J. Phys. Chem. A* **2006**, *110*, 1881−1893.
(26) Veghte, D. P.; Altaf, M. B.; Freedman, M. A. Size Dependence of the Structure of Organic Aerosol. *J. Am. Chem. Soc.* **2013**, *135*, 16046−16049.
(27) Zuend, A.; Seinfeld, J. H. Modeling the Gas-Particle Partitioning of Secondary Organic Aerosol: The Importance of Liquid-Liquid Phase Separation. *Atmos. Chem. Phys.* **2012**, *12*, 3857−3882.
(28) Ott, E.-J. E.; Tackman, E. C.; Freedman, M. A. Effects of Sucrose on Phase Transitions of Organic/Inorganic Aerosols. *ACS Earth Space Chem.* **2020**, *4*, 591−601.
(29) You, Y.; Renbaum-Wolff, L.; Carreras-Sospedra, M.; Hanna, S. J.; Hiranuma, N.; Kamal, S.; Smith, M. L.; Zhang, X.; Weber, R. J.; Shilling, J. E.; et al. Images Reveal That Atmospheric Particles Can Undergo Liquid−Liquid Phase Separations. *Proc. Natl. Acad. Sci. U.S.A.* **2012**, *109*, 13188−13193.
(30) Hodas, N.; Zuend, A.; Mui, W.; Flagan, R. C.; Seinfeld, J. H. Influence of Particle-Phase State on the Hygroscopic Behavior of Mixed Organic−Inorganic Aerosols. *Atmos. Chem. Phys.* **2015**, *15*, 5027−5045.
(31) Razafindrambinina, P. N.; Malek, K. A.; Dawson, J. N.; DiMonte, K.; Raymond, T. M.; Dutcher, D. D.; Freedman, M. A.; Asa-Awuku, A. Hygroscopicity of Internally Mixed Ammonium Sulfate and Secondary Organic Aerosol Particles Formed at Low and High Relative Humidity. *Environ. Sci.: Atmos.* **2022**, *2*, 202−214.
(32) Massoli, P.; Lambe, A. T.; Ahern, A. T.; Williams, L. R.; Ehn, M.; Mikkilä, J.; Canagaratna, M. R.; Brune, W. H.; Onasch, T. B.; Jayne, J. T. , et al. Relationship between Aerosol Oxidation Level and Hygroscopic Properties of Laboratory Generated Secondary Organic Aerosol (SOA) Particles. *Geophys. Res. Lett.* **2010**, *3724*, DOI: 10.1029/2010gl045258,
(33) Vu, D.; Gao, S.; Berte, T.; Kacarab, M.; Yao, Q.; Vafai, K.; Asa-Awuku, A. External and Internal Cloud Condensation Nuclei (CCN) Mixtures: Controlled Laboratory Studies of Varying Mixing States. *Atmos. Meas. Tech.* **2019**, *12*, 4277−4289.
(34) Fofie, E. A.; Donahue, N. M.; Asa-Awuku, A. Cloud Condensation Nuclei Activity and Droplet Formation of Primary and Secondary Organic Aerosol Mixtures. *Aerosol Sci. Technol.* **2018**, *52*, 242−251.
(35) Lee, W.-C.; Deng, Y.; Zhou, R.; Itoh, M.; Mochida, M.; Kuwata, M. Water Solubility Distribution of Organic Matter Accounts for the Discrepancy in Hygroscopicity among Sub-and Supersaturated Humidity Regimes. *Environ. Sci. Technol.* **2022**, *56*, 17924−17935.
(36) Huang, Y.; Mahrt, F.; Xu, S.; Shiraiwa, M.; Zuend, A.; Bertram, A. K. Coexistence of Three Liquid Phases in Individual Atmospheric Aerosol Particles. *Proc. Natl. Acad. Sci. U.S.A.* **2021**, *118*, No. e2102512118.
(37) Han, S.; Hong, J.; Luo, Q.; Xu, H.; Tan, H.; Wang, Q.; Tao, J.; Zhou, Y.; Peng, L.; He, Y.; et al. Hygroscopicity of Organic Compounds as a Function of Organic Functionality, Water Solubility, Molecular Weight, and Oxidation Level. *Atmos. Chem. Phys.* **2022**, *22*, 3985−4004.
(38) Renbaum-Wolff, L.; Song, M.; Marcolli, C.; Zhang, Y.; Liu, P. F.; Grayson, J. W.; Geiger, F. M.; Martin, S. T.; Bertram, A. K. Observations and implications of liquid−liquid phase separation at high relative humidities in secondary organic material produced by <i>α</i>-pinene ozonolysis without inorganic salts. *Atmos. Chem. Phys.* **2016**, *16*, 7969−7979.
(39) Berkemeier, T.; Shiraiwa, M.; Pöschl, U.; Koop, T. Competition between Water Uptake and Ice Nucleation by Glassy Organic Aerosol Particles. *Atmos. Chem. Phys.* **2014**, *14*, 12513−12531.
(40) Gohil, K.; Mao, C.-N.; Rastogi, D.; Peng, C.; Tang, M.; Asa-Awuku, A. Hybrid Water Adsorption and Solubility Partitioning for Aerosol Hygroscopicity and Droplet Growth. *Atmos. Chem. Phys. Discuss.* **2022**, *22*, 12769−12787.
(41) Nakao, S. Why Would Apparent κ Linearly Change with O/C? Assessing the Role of Volatility, Solubility, and Surface Activity of Organic Aerosols. *Aerosol Sci. Technol.* **2017**, *51*, 1377−1388.
(42) Jimenez, J. L.; Canagaratna, M. R.; Donahue, N. M.; Prevot, A. S. H.; Zhang, Q.; Kroll, J. H.; DeCarlo, P. F.; Allan, J. D.; Coe, H.; Ng, N. L.; Aiken, A. C.; Docherty, K. S.; Ulbrich, I. M.; Grieshop, A. P.; Robinson, A. L.; Duplissy, J.; Smith, J. D.; Wilson, K. R.; Lanz, V. A.; Hueglin, C.; Sun, Y. L.; Tian, J.; Laaksonen, A.; Raatikainen, T.; Rautiainen, J.; Vaattovaara, P.; Ehn, M.; Kulmala, M.; Tomlinson, J. M.; Collins, D. R.; Cubison, M. J.; Dunlea, J.; Huffman, J. A.; Onasch, T. B.; Alfarra, M. R.; Williams, P. I.; Bower, K.; Kondo, Y.; Schneider, J.; Drewnick, F.; Borrmann, S.; Weimer, S.; Demerjian, K.; Salcedo, D.; Cottrell, L.; Griffin, R.; Takami, A.; Miyoshi, T.; Hatakeyama, S.; Shimono, A.; Sun, J. Y.; Zhang, Y. M.; Dzepina, K.; Kimmel, J. R.; Sueper, D.; Jayne, J. T.; Herndon, S. C.; Trimborn, A. M.; Williams, L. R.; Wood, E. C.; Middlebrook, A. M.; Kolb, C. E.; Baltensperger, U.; Worsnop, D. R.; et al. Evolution of Organic Aerosols in the Atmosphere. *Science* **2009**, *326*, 1525−1529.
(43) Tang, X.; Cocker, D. R.; Asa-Awuku, A. Are Sesquiterpenes a Good Source of Secondary Organic Cloud Condensation Nuclei

(CCN)? Revisiting β-Caryophyllene CCN. *Atmos. Chem. Phys.* **2012**, *12*, 8377−8388.
(44) Lambe, A. T.; Onasch, T. B.; Massoli, P.; Croasdale, D. R.; Wright, J. P.; Ahern, A. T.; Williams, L. R.; Worsnop, D. R.; Brune, W. H.; Davidovits, P. Laboratory Studies of the Chemical Composition and Cloud Condensation Nuclei (CCN) Activity of Secondary Organic Aerosol (SOA) and Oxidized Primary Organic Aerosol (OPOA). *Atmos. Chem. Phys.* **2011**, *11*, 8913−8928.
(45) Song, M.; Marcolli, C.; Krieger, U. K.; Zuend, A.; Peter, T. Liquid-Liquid Phase Separation and Morphology of Internally Mixed Dicarboxylic Acids/Ammonium Sulfate/Water Particles. *Atmos. Chem. Phys.* **2012**, *12*, 2691−2712.
(46) Petters, M. D.; Kreidenweis, S. M. A Single Parameter Representation of Hygroscopic Growth and Cloud Condensation Nucleus Activity−Part 2: Including Solubility. *Atmos. Chem. Phys.* **2008**, *8*, 6273−6279.
(47) Riipinen, I.; Rastak, N.; Pandis, S. N. Connecting the Solubility and CCN Activation of Complex Organic Aerosols: A Theoretical Study Using Solubility Distributions. *Atmos. Chem. Phys.* **2015**, *15*, 6305−6322.
(48) Altaf, M. B.; Zuend, A.; Freedman, M. A. Role of Nucleation Mechanism on the Size Dependent Morphology of Organic Aerosol. *Chem. Commun.* **2016**, *52*, 9220−9223.
(49) Reid, J. P.; Dennis-Smither, B. J.; Kwamena, N.-O. A.; Miles, R. E. H.; Hanford, K. L.; Homer, C. J. The Morphology of Aerosol Particles Consisting of Hydrophobic and Hydrophilic Phases: Hydrocarbons, Alcohols and Fatty Acids as the Hydrophobic Component. *Phys. Chem. Chem. Phys.* **2011**, *13*, 15559−15572.
(50) Freedman, M. A. Liquid−Liquid Phase Separation in Supermicrometer and Submicrometer Aerosol Particles. *Acc. Chem. Res.* **2020**, *53*, 1102−1110.
(51) Kuwata, M.; Shao, W.; Lebouteiller, R.; Martin, S. T. Classifying Organic Materials by Oxygen-to-Carbon Elemental Ratio to Predict the Activation Regime of Cloud Condensation Nuclei (CCN). *Atmos. Chem. Phys.* **2013**, *13*, 5309−5324.
(52) Wong, J. P. S.; Lee, A. K. Y.; Slowik, J. G.; Cziczo, D. J.; Leaitch, W. R.; Macdonald, A.; Abbatt, J. P. D. Oxidation of Ambient Biogenic Secondary Organic Aerosol by Hydroxyl Radicals: Effects on Cloud Condensation Nuclei Activity. *Geophys. Res. Lett.* **2011**, *38* 22, DOI: 10.1029/2011gl049351,
(53) Alfarra, M. R.; Good, N.; Wyche, K. P.; Hamilton, J. F.; Monks, P. S.; Lewis, A. C.; Mcfiggans, G. Water Uptake Is Independent of the Inferred Composition of Secondary Aerosols Derived from Multiple Biogenic VOCs. *Atmos. Chem. Phys.* **2013**, *13*, 11769−11789.
(54) Chang, R. Y. W.; Slowik, J. G.; Shantz, N. C.; Vlasenko, A.; Liggio, J.; Sjostedt, S. J.; Leaitch, W. R.; Abbatt, J. P. D. The Hygroscopicity Parameter (κ) of Ambient Organic Aerosol at a Field Site Subject to Biogenic and Anthropogenic Influences: Relationship to Degree of Aerosol Oxidation. *Atmos. Chem. Phys.* **2010**, *10*, 5047−5064.
(55) Suda, S. R.; Petters, M. D.; Yeh, G. K.; Strollo, C.; Matsunaga, A.; Faulhaber, A.; Ziemann, P. J.; Prenni, A. J.; Carrico, C. M.; Sullivan, R. C.; et al. Influence of Functional Groups on Organic Aerosol Cloud Condensation Nucleus Activity. *Environ. Sci. Technol.* **2014**, *48*, 10182−10190.
(56) Farmer, D. K.; Cappa, C. D.; Kreidenweis, S. M. Atmospheric Processes and Their Controlling Influence on Cloud Condensation Nuclei Activity. *Chem. Rev.* **2015**, *115*, 4199−4217.
(57) You, Y.; Smith, M. L.; Song, M.; Martin, S. T.; Bertram, A. K. Liquid−Liquid Phase Separation in Atmospherically Relevant Particles Consisting of Organic Species and Inorganic Salts. *Int. Rev. Phys. Chem.* **2014**, *33*, 43−77.
(58) Chang, E. I.; Pankow, J. F. Prediction of Activity Coefficients in Liquid Aerosol Particles Containing Organic Compounds, Dissolved Inorganic Salts, and Water—Part 2: Consideration of Phase Separation Effects by an X-UNIFAC Model. *Atmos. Environ.* **2006**, *40*, 6422−6436.
(59) Gorkowski, K.; Preston, T. C.; Zuend, A. Relative-Humidity-Dependent Organic Aerosol Thermodynamics via an Efficient Reduced-Complexity Model. *Atmos. Chem. Phys.* **2019**, *19*, 13383−13407.
(60) Ovadnevaite, J.; Zuend, A.; Laaksonen, A.; Sanchez, K. J.; Roberts, G.; Ceburnis, D.; Decesari, S.; Rinaldi, M.; Hodas, N.; Facchini, M. C.; et al. Surface Tension Prevails over Solute Effect in Organic-Influenced Cloud Droplet Activation. *Nature* **2017**, *546*, 637−641.
(61) Lam, H. K.; Xu, R.; Choczynski, J.; Davies, J. F.; Ham, D.; Song, M.; Zuend, A.; Li, W.; Tse, Y.-L. S.; Chan, M. N. Effects of Liquid−Liquid Phase Separation and Relative Humidity on the Heterogeneous OH Oxidation of Inorganic−Organic Aerosols: Insights from Methylglutaric Acid and Ammonium Sulfate Particles. *Atmos. Chem. Phys.* **2021**, *21*, 2053−2066.
(62) Kundu, S.; Kawamura, K.; Kobayashi, M.; Tachibana, E.; Lee, M.; Fu, P. Q.; Jung, J. A Sub-Decadal Trend in Diacids in Atmospheric Aerosols in Eastern Asia. *Atmos. Chem. Phys.* **2016**, *16*, 585−596.
(63) Li, X.; Yang, Z.; Fu, P.; Yu, J.; Lang, Y.; Liu, D.; Ono, K.; Kawamura, K. High abundances of dicarboxylic acids, oxocarboxylic acids, and α-dicarbonyls in fine aerosols (PM2.5) in Chengdu, China during wintertime haze pollution. *Environ. Sci. Pollut. Res.* **2015**, *22*, 12902−12918.
(64) Lance, S.; Nenes, A.; Medina, J.; Smith, J. N. Mapping the Operation of the DMT Continuous Flow CCN Counter. *Aerosol Sci. Technol.* **2006**, *40*, 242−254.
(65) Roberts, G. C.; Nenes, A. A Continuous-Flow Streamwise Thermal-Gradient CCN Chamber for Atmospheric Measurements. *Aerosol Sci. Technol.* **2005**, *39*, 206−221.
(66) Engelhart, G. J.; Asa-Awuku, A.; Nenes, A.; Pandis, S. N. CCN Activity and Droplet Growth Kinetics of Fresh and Aged Monoterpene Secondary Organic Aerosol. *Atmos. Chem. Phys.* **2008**, *8*, 3937−3949.
(67) Moore, R. H.; Nenes, A.; Medina, J. Scanning Mobility CCN Analysis-A Method for Fast Measurements of Size-Resolved CCN Distributions and Activation Kinetics. *Aerosol Sci. Technol.* **2010**, *44*, 861−871.
(68) Tang, X.; Price, D.; Praske, E.; Vu, D. N.; Purvis-Roberts, K.; Silva, P. J.; Cocker III, D. R.; Asa-Awuku, A. Cloud Condensation Nuclei (CCN) Activity of Aliphatic Amine Secondary Aerosol. *Atmos. Chem. Phys.* **2014**, *14*, 5959−5967.
(69) Barati, F.; Yao, Q.; Asa-Awuku, A. A. Insight into the Role of Water-Soluble Organic Solvents for the Cloud Condensation Nuclei Activation of Cholesterol. *ACS Earth Space Chem.* **2019**, *3*, 1697−1705.
(70) Wiedensohler, A. An Approximation of the Bipolar Charge Distribution for Particles in the Submicron Size Range. *J. Aerosol Sci.* **1988**, *19*, 387−389.
(71) Petters, M. D.; Kreidenweis, S. M. A Single Parameter Representation of Hygroscopic Growth and Cloud Condensation Nucleus Activity. *Atmos. Chem. Phys.* **2007**, *7*, 1961−1971.
(72) Dawson, J. N.; Malek, K. A.; Razafindrambinina, P. N.; Raymond, T. M.; Dutcher, D. D.; Asa-Awuku, A. A.; Freedman, M. A. Direct Comparison of the Submicron Aerosol Hygroscopicity of Water-Soluble Sugars. *ACS Earth Space Chem.* **2020**, *4*, 2215−2226.
(73) Marsh, A.; Miles, R. E. H.; Rovelli, G.; Cowling, A. G.; Nandy, L.; Dutcher, C. S.; Reid, J. P. Influence of Organic Compound Functionality on Aerosol Hygroscopicity: Dicarboxylic Acids, Alkyl-Substituents, Sugars and Amino Acids. *Atmos. Chem. Phys.* **2017**, *17*, 5583−5599.
(74) Prenni, A. J.; Petters, M. D.; Kreidenweis, S. M.; DeMott, P. J.; Ziemann, P. J. Cloud Droplet Activation of Secondary Organic Aerosol. *J. Geophys. Res.: Atmos.* **2007**, *112* D10. DOI: DOI: 10.1029/2006JD007963.
(75) Wex, H.; Petters, M. D.; Carrico, C. M.; Hallbauer, E.; Massling, A.; McMeeking, G. R.; Poulain, L.; Wu, Z.; Kreidenweis, S. M.; Stratmann, F. Towards Closing the Gap between Hygroscopic Growth and Activation for Secondary Organic Aerosol: Part 1-Evidence from Measurements. *Atmos. Chem. Phys.* **2009**, *9*, 3987−3997.

(76) Jurányi, Z.; Gysel, M.; Duplissy, J.; Weingartner, E.; Tritscher, T.; Dommen, J.; Henning, S.; Ziese, M.; Kiselev, A.; Stratmann, F.; et al. Influence of gas-to-particle partitioning on the hygroscopic and droplet activation behaviour of α-pinene secondary organic aerosol. *Phys. Chem. Chem. Phys.* **2009**, *11*, 8091−8097.
(77) Pajunoja, A.; Lambe, A. T.; Hakala, J.; Rastak, N.; Cummings, M. J.; Brogan, J. F.; Hao, L.; Paramonov, M.; Hong, J.; Prisle, N. L.; Malila, J.; Romakkaniemi, S.; Lehtinen, K. E. J.; Laaksonen, A.; Kulmala, M.; Massoli, P.; Onasch, T. B.; Donahue, N. M.; Riipinen, I.; Davidovits, P.; Worsnop, D. R.; Petäjä, T.; Virtanen, A. Adsorptive Uptake of Water by Semisolid Secondary Organic Aerosols. *Geophys. Res. Lett.* **2015**, *42*, 3063−3068.
(78) Malek, K. A.; Gohil, K.; Al-Abadleh, H. A.; Asa-Awuku, A. A. Hygroscopicity of Polycatechol and Polyguaiacol Secondary Organic Aerosol in Sub-and Supersaturated Water Vapor Environments. *Environ. Sci.: Atmos.* **2022**, *2*, 24−33.
(79) Razafindrambinina, P. N.; Malek, K. A.; DiMonte, K.; Dawson, J. N.; Raymond, T. M.; Dutcher, D. D.; Freedman, M. A.; Asa-Awuku, A. A. Effects of Mixing State on Water-Uptake Properties of Ammonium Sulfate−Organic Mixtures. *Aerosol Sci. Technol.* **2022**, *56*, 1009−1021.
(80) Good, N.; Topping, D. O.; Duplissy, J.; Gysel, M.; Meyer, N. K.; Metzger, A.; Turner, S. F.; Baltensperger, U.; Ristovski, Z.; Weingartner, E.; Coe, H.; McFiggans, G. Widening the Gap between Measurement and Modelling of Secondary Organic Aerosol Properties? *Atmos. Chem. Phys.* **2010**, *10*, 2577−2593.
(81) Giordano, M. R.; Short, D. Z.; Hosseini, S.; Lichtenberg, W.; Asa-Awuku, A. A. Changes in Droplet Surface Tension Affect the Observed Hygroscopicity of Photochemically Aged Biomass Burning Aerosol. *Environ. Sci. Technol.* **2013**, *47*, 10980−10986.
(82) Chenyakin, Y.; Ullmann, D. A.; Evoy, E.; Renbaum-Wolff, L.; Kamal, S.; Bertram, A. K. Diffusion Coefficients of Organic Molecules in Sucrose−Water Solutions and Comparison with Stokes−Einstein Predictions. *Atmos. Chem. Phys.* **2017**, *17*, 2423−2435.
(83) Hodas, N.; Zuend, A.; Schilling, K.; Berkemeier, T.; Shiraiwa, M.; Flagan, R. C.; Seinfeld, J. H. Discontinuities in Hygroscopic Growth below and above Water Saturation for Laboratory Surrogates of Oligomers in Organic Atmospheric Aerosols. *Atmos. Chem. Phys.* **2016**, *16*, 12767−12792.
(84) Petters, S. S.; Pagonis, D.; Claflin, M. S.; Levin, E. J. T.; Petters, M. D.; Ziemann, P. J.; Kreidenweis, S. M. Hygroscopicity of Organic Compounds as a Function of Carbon Chain Length and Carboxyl, Hydroperoxy, and Carbonyl Functional Groups. *J. Phys. Chem. A* **2017**, *121*, 5164−5174.
(85) Petters, M. D.; Kreidenweis, S. M.; Snider, J. R.; Koehler, K. A.; Wang, Q.; Prenni, A. J.; Demott, P. J. Cloud Droplet Activation of Polymerized Organic Aerosol. *Tellus B* **2006**, *58*, 196−205.
(86) VanReken, T. M.; Ng, N. L.; Flagan, R. C.; Seinfeld, J. H. Cloud Condensation Nucleus Activation Properties of Biogenic Secondary Organic Aerosol. *J. Geophys. Res.: Atmos.* **2005**, *110*, D07206.
(87) Petters, M. D.; Kreidenweis, S. M.; Snider, J. R.; Koehler, K. A.; Wang, Q.; Prenni, A. J.; Demott, P. J. Cloud Droplet Activation of Polymerized Organic Aerosol. *Tellus B* **2006**, *58*, 196−205.
(88) Mao, C.-N.; Malek, K. A.; Asa-Awuku, A. Hygroscopicity and the Water-Polymer Interaction Parameter of Nano-Sized Biodegradable Hydrophilic Substances. *Aerosol Sci. Technol.* **2021**, *55*, 1115−1124.

https://doi.org/10.1021/acsenvironau.3c00015
ACS Environ. Au 2023, 3, 348−360